Vol 18 No 11, November 2009
1674-1056/2009/18(11)/5084-07

Chinese Physics B

© 2009 Chin. Phys. Soc.
and IOP Publishing Ltd

Refractivity estimation from radar sea clutter*

Huang Si-Xun(黄思训)†, Zhao Xiao-Feng(赵小峰), and Sheng Zheng(盛 峥)

Institute of Meteorology, PLA University of Science & Technology, Nanjing 211101, *China*

(Received 21 December 2008; revised manuscript received 13 March 2009)

This paper addresses the problem of estimating lower atmospheric refractivity under the nonstandard propagation conditions frequently encountered in low altitude maritime radar applications. The vertical structure of the refractive environment is modeled by using a five-parameter model, and the horizontal structure is modeled as range-independent. The electromagnetic propagation in the troposphere is simulated by using a split-step fast Fourier transform based on parabolic approximation to the wave equation. A global search marked as a modified genetic algorithm (MGA) for the 5 environmental parameters is performed by using a genetic algorithm (GA) integrated with a simulated annealing technique. The retrieved results from simulated runs demonstrate the ability of this method to make atmospheric refractivity estimations. A comparison with the classical GA and the Bayesian Markov Chain Monte Carlo (Bayesian-MCMC) technique shows that the MGA can not only shorten the inverse time but also improve the inverse precision. For real data cases, the inversion values do not match the reference data very well. The inverted profile, however, can be used to synoptically describe the real refractive structure.

Keywords: atmosphere duct, parabolic wave equation, refractivity from clutter

PACC: 9260V

1. Introduction

Atmosphere ducts can cause electromagnetic wave propagation paths and effective coverage areas to be different from those under standard conditions,[1] which affects the performance of electric systems as well as tactical selection and disposition. A signal sent from a surface or low altitude source, such as a ship or low-flying object, can be totally trapped inside the duct. This will result in multiple reflections from the surface and they will appear as clutter rings in the radar plan position indicator screen (Fig.1). The desirability of not having to use additional equipment to estimate refractivity motivates the estimation of range and height variation about refractivity from clutter (RFC).[2] The RFC refers to techniques that estimate the atmospheric refractivity profile from returns of radar clutter. Gerstoft and his colleagues have tried to apply various inversion algorithms, such as a genetic algorithm (GA),[3] sequential importance sampling,[4] and a Kalman filter,[5] to estimate refractive structure and they have achieved some delightful fruit. Their latest work can be consulted in Ref.[6]. In our country, however, very few studies in this field are published in literature and books. In our previous work, several numerical simulations were performed. The anti-noise capability of GA for RFC was discussed in Ref.[7], where simulated results could provide some useful information for practice inversion. Then we introduced the Bayesian-Markov Chain Monte Carlo (Bayesian-MCMC) method to retrieve refractivity parameters.[8] Although it is slower than GA, the probability densities obtained by this method are closer to the true distribution. Observation weight of propagation loss was also considered in Ref.[9]. Simulation values show that exponent expression can perfectly describe the variety of observation weight with distance, and a reasonable observation weight can preferably improve retrieval speed and precision.

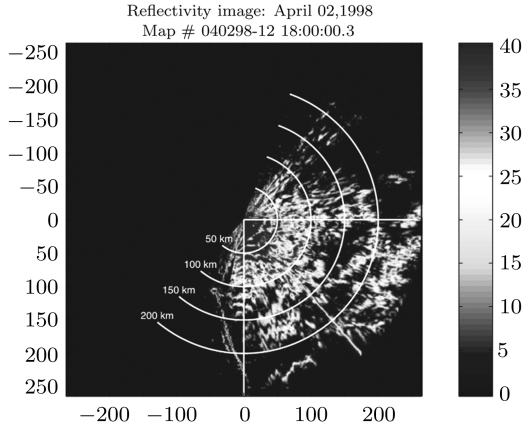


Fig.1. Plan position indicator data (dB) from SPANDAR radar corresponding to Wallops run 12 (Gersoft, 2003).

*Project supported by the National Natural Science Foundation of China(Grant No 40775025).

†Corresponding author. E-mail: huangsxp@yahoo.com.cn

In this paper, we introduce a simulated annealing (SA) technique to ameliorate GA and combine a global search scheme with a divisive search scheme. The inversion algorithm is implemented both on simulated data and real radar sea clutter from Wallops Island, Virginia. Reference data are from range-dependent refractivity profiles obtained with a helicopter. In order to simplify the inversion process, however, the refractive structure is assumed to be range-independent. The retrieved values demonstrate the feasibility of this approach to estimate environmental refractive structure from radar data itself and the range-independent hypothesis is reasonable for the marine environment in the case considered by this paper.

2. Forward modeling and inversion algorithm

2.1. Propagation model

The most commonly used approach to model wave propagation in the troposphere is the Fourier split-step solution to the parabolic equation.[10] This numerical solution is a forward solver with the ability to handle vertical and horizontal inhomogeneities in the refractive profile and is capable of delivering accurate propagation loss estimates in complicated environments.

Let $u(x_k, z)$ be the electric field at range x_k and height z Then the field at range x_{k+1} and height z, denoted by $u(x_{k+1}, z)$, is given by the Fourier split-step solution to the parabolic wave equation,[11]

$$\begin{aligned} & u(x_{k+1}, z) \\ = & \exp\left\{\mathrm{i}\frac{k_0[m^2-1]}{2}\cdot\delta x\right\} \\ & \times F^{-1}\left(\exp\left(-\mathrm{i}\frac{p^2\cdot\delta x}{2k_0}\right)\cdot F\left\{u(x_k, z)\right\}\right), \end{aligned} \quad (1)$$

where F and F^{-1} are the spatial forward and inverse Fourier transform along the height z, $\delta x = x_{k+1} - x_k$ is the range increment. $m = n(1 + z/a_{\mathrm{E}})$ is the modified refractive index, in which n is the index of refraction, and a_{E} is the radius of the Earth, k_0 is the wave number, p is the transform variable often referred to as the vertical wave number or spatial frequency.

Based on Eq.(1), the one-way propagation loss L in dB is determined by taking the difference between the free space loss and the propagation factor, Q[12]

$$L = 20\log_{10}\left(\frac{4\pi r}{\lambda}\right) - 20\log_{10}(Q). \quad (2)$$

The first term in Eq.(2) is the free space loss, where r is the range and λ is the wavelength. The propagation factor Q could be expressed as

$$Q = \sqrt{x}\cdot|u(x, z)|. \quad (3)$$

2.2. Radar model

The received power P_{c} from radar sea clutter could be calculated as[13]

$$P_{\mathrm{c}} = \frac{4\pi P_{\mathrm{t}} G_{\mathrm{t}} G_{\mathrm{r}} A_{\mathrm{c}} \sigma^{\mathrm{o}}}{L^2\lambda^2}, \quad (4)$$

where P_{t} is the transmitted power, G_{t} and G_{r} are the transmitting and receiving antenna gains respectively, λ is the wavelength, A_{c} is the illuminated area and σ^{o} is the sea clutter's normalized radar cross section. At low grazing angles, A_{c} is a linear function of range r, thus Eq.(4) can be rewritten as[3]

$$P_{\mathrm{c}} = \frac{C\sigma^{\mathrm{o}} r}{L^2}, \quad (5)$$

where C accounts for all of the constant terms in Eq.(4). Letting the symbols P_{c}, C, σ^{o} and L represent the associated values in dB as opposed to real numbers, we can model the received signal power from the clutter as[3]

$$P_{\mathrm{c}} = -2L + 10\log_{10}(r) + \sigma^{\mathrm{o}} + C, \quad (6)$$

here, some stochastic variations in range as a Markov process are simulated as noise.

2.3. Environmental model

A five-parameter refractivity model has been proposed by the Naval Force Physics Laboratory in California and can be described as[14]

$$m = (\delta, c_1, z_{\mathrm{b}}, z_{\mathrm{thick}}, M_{\mathrm{d}})^{\mathrm{T}}, \quad (7)$$

where δ is the evaporation duct height, c_1 is the slope in the mixed layer, z_{b} is the trapping-layer base height, z_{thick} is the thickness of the inversion layer, and M_{d} is the M deficit of the inversion layer.

The value of modified refractivity as a function of height z is given by[3]

$$M(z) = M_0 + \begin{cases} M_1 + c_0\left(z - \delta \log \dfrac{z}{z_0}\right), & \text{for } z < z_{\rm d}, \\ c_1 z, & \text{for } z_{\rm d} < z < z_{\rm b}, \\ c_1 z_{\rm b} - M_{\rm d}\dfrac{z - z_{\rm b}}{z_{\rm thick}}, & \text{for } z_{\rm b} < z < z_{\rm t}, \\ c_1 z_{\rm b} - M_{\rm d} + c_2(z - z_{\rm t}), & \text{for } z_{\rm t} < z. \end{cases} \tag{8}$$

In practical implementations, prior information might be available from a variety of sources (e.g., numerical weather prediction models, atmospheric soundings, etc.) that could improve the quality of the inverse problem solutions. The boundary of refractivity parameters is shown in Table 1 (for a detailed description refer to Ref.[3]).

Table 1. Parameter search bounds for the five-parameter model.

parameter/unit	lower Bound	upper Bound
thickness/m	0	100
M-deficit/M-units	0	100
mixed layer slope/(M-units/m)	–1	0.4
evaporation duct height/m	0	40
base height/m	3	300

2.4. Radar and reference data

The data presented in Fig.1 are from a surface-based ducting event that occurred at April 1998. Radar data were obtained by using the space range radar (SPANDAR). The radar's system parameters as configured for the data taken here are shown in Table 2.

Table 2. Space range radar parameters.

parameter/unit	measurement
frequency/GHz	2.84
power/dB	91.40
beamwidth/(°)	0.39
antenna gain/dB	52.80
height/m	30.78
polarization	vertical
Range bin width/m	600

Meteorological soundings were obtained by an instrumented helicopter which would fly in and out on the 150deg radial from a point 4 km due east of the SPANDAR. A contour plot of modified refractivity versus range and height is shown in Fig.2. The figure illustrates that the profiles show some range dependency, which indicates that for inversion a range-dependent model might be needed. In order to simplify the inverse process, however, in this paper, the environment is assumed to be horizontally homogeneous.

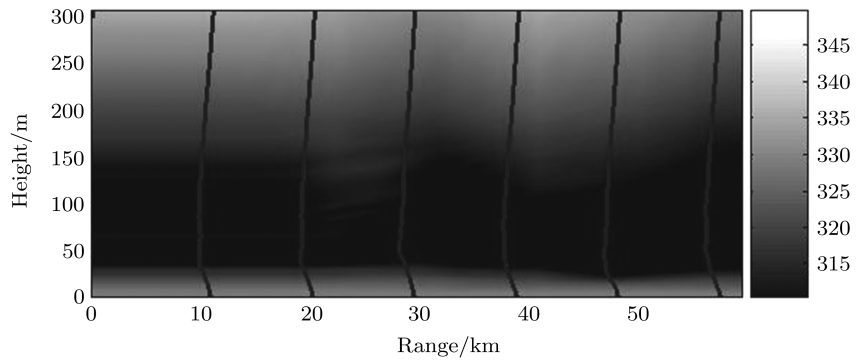


Fig.2. Contour plot of modified refractivity profiles (M-units) measured from a helicopter.

2.5. Inversion algorithm

In the RFC problem, using GA and Bayesian-MCMC to perform a global search is computationally too expensive.[3,7,8] This advances the modified GA (MGA) for the 5 environmental parameter inversion, which is performed by using GA associated with the simulated annealing technique and combining the global search scheme with a divisive search scheme. In the divisive search process, all parameters are kept unchanged except the ith; the ith parameter is treated with selection and mutation, but the others are treated only with mutation. The flow chart is shown in Fig.3.

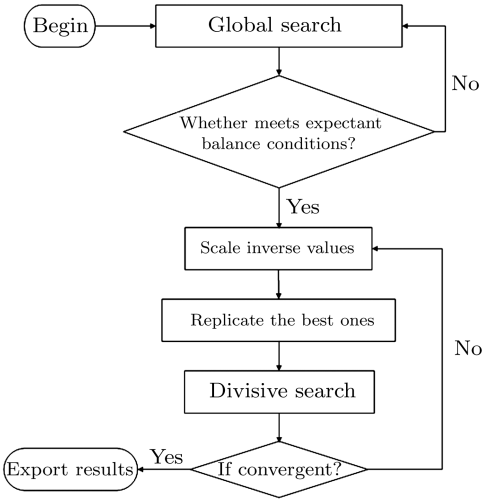


Fig.3. The flow chart of MGA.

The GA search parameters are: parameter quantization 1024 values; population size 100; reproduction size 0.1; crossover probability 0.5; general mutation probability 0.01; creep mutation size 0.16. For further information about the application of GA for parameter estimation refer to Refs.[15] and [16].

3. Numerical experiments

Note the refractive information measured by helicopter as $m^{\rm obs}$, and the radar sea clutter data corresponding to the discrete ranges of interest as $P_{\rm c}^{\rm obs}$. The inverted refractivity parameters are described as $m^{\rm inv}$, and the signal power calculated basing on $m^{\rm inv}$ are noted as $P_{\rm c}(m^{\rm inv})$. It is assumed that the difference between the observed $P_{\rm c}^{\rm obs}$ and modeled $P_{\rm c}(m^{\rm inv})$ clutter is Gaussian. This leads to a simple least squares objective function,

$$\phi(m^{\rm inv}) = e^{\rm T} e, \tag{9}$$

where

$$e = P_{\rm c}^{\rm obs} - P_{\rm c}(m^{\rm inv}) - \hat{T}, \tag{10}$$

$$\hat{T} = \bar{P}_{\rm c}^{\rm obs} - \bar{P}_{\rm c}(m^{\rm inv}), \tag{11}$$

and the bar denotes the mean across the elements in the vector. $\hat{T}$ is an estimated normalization constant for each realization of $m^{\rm inv}$.

3.1. Simulation results

Without variations, Fig.4(a) gives the retrieved modified refractivity profile along with the simulated true value and the corresponding propagation loss values are shown in Fig.4(b). The solid line simulates the true values and the dash-dotted line denotes the inverted values. For radar system parameters refer to Ref.[7].

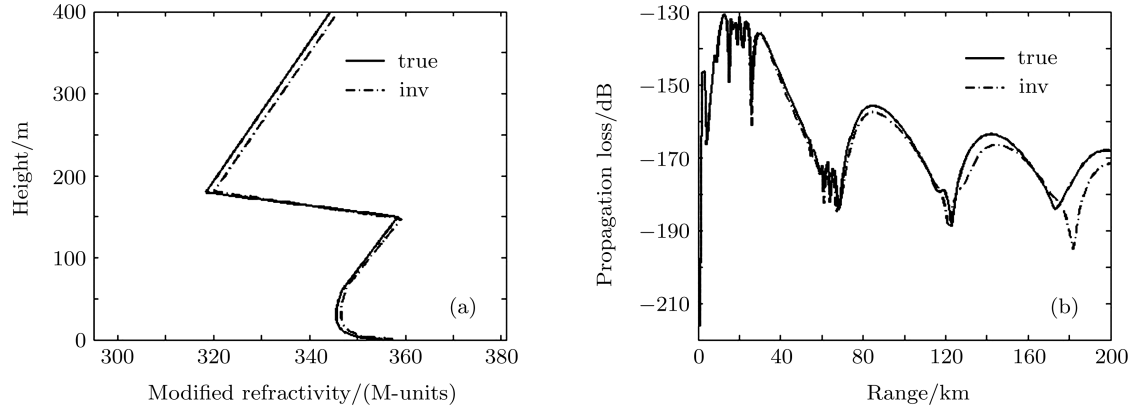


Fig.4. (a) Simulated and inverted modified refractivity profile, (b) simulated and inverted propagation loss.

From the results given by Fig.4, some conclusions can be obtained: 1) the inverted results show a perfect match with the true values, which indicates that the algorithm could be used to retrieve refractivity parameters; 2) compared with the results in our previous work,[7,8] the results presented here are more accurate; 3) although the estimated propagation loss values have a tendency to deviate from the true values along with range extension, within 60 kilometers, they display good agreement.

Table 3 describes the detailed refractivity parameter values retrieved by MGA, GA and Bayesian-MCMC. This gives the inverted results of the 5000th generation retrieved by GA and Bayesian-MCMC but only the 1000th generation by MGA (for the results of GA and Bayesian-MCMC refer to Refs.[7] and [8]). It is obviously seen that the precision and the efficiency of MGA are higher than GA and Bayesian-MCMC. For mixed layer slope c_1 in particular, which is important for precision improvement, MGA could retrieve more accurate values.

Table 3. Performance comparison of MGA and GA and Bayesian-MCMC.

	δ/m	c_1/M-units/m	z_b/m	z_{thick}/m	M_d/M-units
true Value	30	0.13	150	30	40
MGA	29.9	0.133	147.4	34.0	39.3
GA	30.6	0.269	152.0	42.4	43.1
Bayesian-MCMC	30.6	0.212	155.4	31.3	42.5

3.2. Real data results

Figure 5(a) summarizes the inversion and assessment of the inversion results. The clutter P_c^{obs} along azimuth 150deg and 10–60 km in range is extracted from the clutter map (Fig.1) and shown as a solid line. The best matching replica is shown as a dash-dotted line, and for reference, the modeled clutter returns from the helicopter profiles are shown as a dashed line. Figure 5(b) shows the best estimated refractivity profiles (dash-dotted line) along with the helicopter refractivity profiles (dashed line). This is on the assumption that the environment is horizontally homogeneous, so the dashed line is constructed with the mean value corresponding to the discrete ranges of interest.

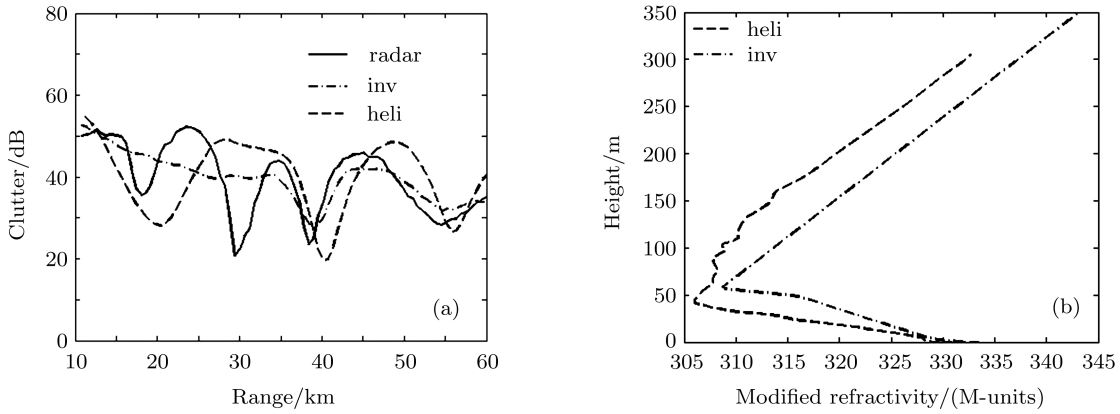


Fig.5. (a) The radar and modeled clutter return (dB). (b) Modified refractivity profiles based on helicopter and inverted values.

The inversion can visually be judged by examining how the peaks in the replica are matched. Based on the location of maxima and minima in Fig.5(a), the inversion only matches well at longer ranges, which is different from the simulated results. There are some reasons for this: first, the simulated values are calculated without variation, and in the real case, there exists a great deal of noise in the radar sea clutter;

second, based on the parabolic equation model, the initial field (i.e. the field at range 0) is calculated by assuming free-space conditions, which is impossible in the real atmospheric environment; third, some stochastic variations in range as a Markov process are simulated, which could strengthen or weaken the noise in the radar sea clutter data. The longer the signal propagates, the more it will counteract the noise effect. Figure 5(b) demonstrates the possibility of using a radar itself for refractive structure estimation by the method presented above. In this paper, the slope of the upper layer is selected as 0.118 M-unit/m. The profiles above the trapping layer, in general, are upward refracting, so this is not a sensitive parameter.

An important issue is to be able to estimate the statistics of posterior propagation loss, which is essential for many radar and communication systems. These environmental statistics can be used to predict the radar performance. Figures 6(a) and 6(b) show the modeled propagation loss for the helicopter profiles and the optimal inverted environment respectively. It is obviously seen that owing to the existence of a surface-based duct, the radar signal is remarkably trapped in the duct, which increases the maximum radar channel range. At the same time, radar is blind to the area above the duct. The difference between these two is displayed in Fig.6(c). The error is controlled within 40 dB, which demonstrates how well the inverted profile is able to predict the propagation loss. Although it is safe to say that horizontally varying environments do occur 14% of the time,[17] in comparison with results given in Ref.[3], the range-independent refractive structure hypothesis will arouse much more error.

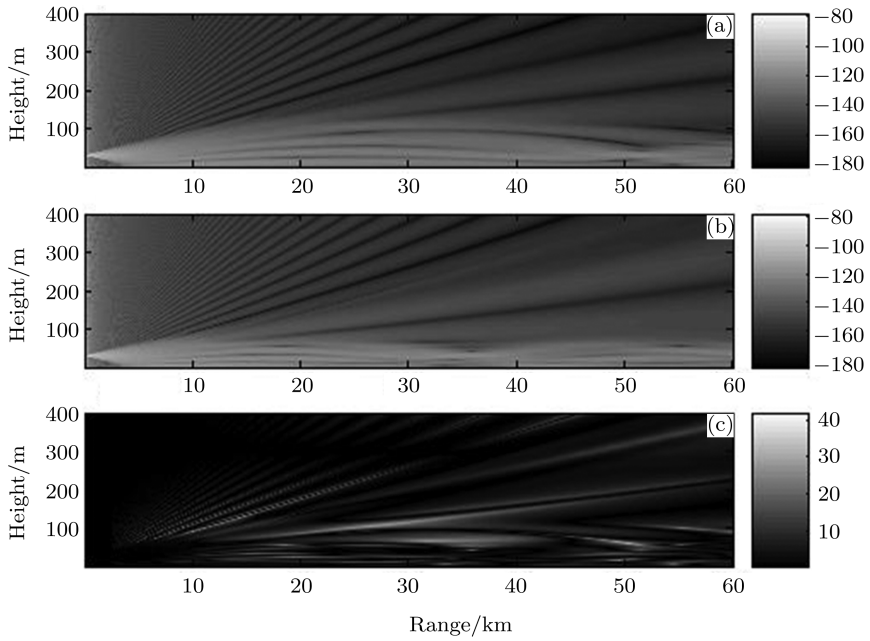


Fig.6. (a) Coverage diagram (dB) based on helicopter profiles, (b) coverage diagram (dB) corresponding to inverted profiles, (c) difference (dB) between coverage diagrams in Figs.6(a) and 6(b).

4. Conclusion

Implementation of the inference of refractivity parameters from radar clutter has been described. An algorithm integrating SA into GA and combining a global search scheme with a divisive search scheme has been proposed. In this paper, we attempt to retrieve the refractivity structure from real sea clutter for the first time. Simulated results and real data inversion values both demonstrate the feasibility of this algorithm for RFC inversion. Because the helicopter data only show a little horizontal variability for the case considered above, the range-independent assumption gives rise to errors that are not large, whereas greater variability is likely to

be encountered in worldwide sampling. Therefore, it is necessary to develop new methods for range-dependent inversion.

Acknowledgment

The authors would like to thank Professor P Gerstoft at the Marine Physical Laboratory, University of California, San Diego, La Jolla, California, USA, for providing the Wallops'98 radar clutter data and corresponding helicopter refractivity measurements.

References

[1] Yan H J, Fu Y and Hong Z J 2006 *Introduction to Modern Atmospheric Refraction* (Shanghai: Science and Educational Press) (in Chinese)

[2] Liu A G, Cha H and Liu F 2007 *Chin. J. Radio Science* **22** 867 (in Chinese)

[3] Gersoft P, Rogers L T, Krolik J K and Hodgkiss W S 2003 *Radio Sci.* **38** 8053

[4] Vasudevan S, Anderson H R, Kraut S Gerstoft P, Rogers L T and Krolik J L 2007 *Radio Sci.* **42** 2014

[5] Yardim C, Gerstoft P and Hodgkiss W S 2008 *IEEE Antennas Propag.* **56** 1058

[6] Douvenot R, Fabbro V, Gerstoft P, Bourlier C and Saillard J 2008 *Radio Sci.* **43** 3842

[7] Sheng Z and Huang S X 2009 *Acta Phys. Sin.* **58** 4328 (in Chinese)

[8] Sheng Z, Huang S X and Zheng G D 2009 *Acta Phys. Sin.* **58** 4335 (in Chinese)

[9] Sheng Z, Huang S X and Zhao X F 2009 *Acta Phys. Sin.* (have accepted) (in Chinese)

[10] Dockery G D 1988 *IEEE Antennas Propag.* **36** 1464

[11] Kuttler J R and Dockery G D 1991 *Radio Sci.* **26** 381

[12] Barrios A E 1997 *Terrain Parabolic Equation Model (TPEM) Computer Software Configuration Item* (CSCI) Documents AD-A 327 522

[13] Jiao P N and Zhang Z Z 2007 *Radar Environment and Electromagnetic Propagation Traits* (Beijing: Publishing House of Electronics Industry) (in Chinese)

[14] Gerstoft P, Rogers L T, Hodgkiss W S and Wagner L J 2003 *IEEE J. Oceanic Eng.* **28** 513

[15] Wang X P and Cao L M 2006 *Genetic Algorithm—Theory, Applications and Software Realization* (Xi'an: Press of Xi'an Jiaotong University) (in Chinese)

[16] Chen G L and Wang X F 1996 *Genetic Algorithm and its Application* (Beijing: People Posting Press) (in Chinese)

[17] Barrios A E 1991 *Radio Wave Propagation in Horizontally Inhomogeneous Environments by Using the Parabolic Equation Method* AD-A 242 082